DALTON
FULL PAPER

A density functional study of ethylene rearrangements assisted by tungsten calix[4]arenes

Simona Fantacci,[a] Antonio Sgamellotti,*[a] Nazzareno Re[b] and Carlo Floriani[c]

[a] *Dipartimento di Chimica e Centro Studi CNR per il Calcolo Intensivo in Scienze Molecolari, Università degli Studi di Perugia, I-06123, Perugia, Italy*
[b] *Facoltà di Farmacia, Università G. D'Annunzio, I-66100, Chieti, Italy*
[c] *Institut de Chimie Minérale et Analitique, BCH, Université de Lausanne, CH-1015, Lausanne, Switzerland*

Received 6th November 2000, Accepted 4th April 2001
First published as an Advance Article on the web 10th May 2001

Density functional calculations have been performed on all complexes involved in the rearrangements undergone by ethylene on the calix[4]arene tungsten fragment. [{*p*-Bu^t-calix[4](O)$_4$}W(η^2-C$_2$H$_4$)], which is the starting reactant of the rearrangement process, has been carefully investigated. In order to reduce the computational effort a simplified model of tungsten calix[4]arene has been considered. Preliminary calculations have shown that four vinylate groups reproduce adequately the geometrical, electronic, and bonding parameters of the calix[4]arene ligand so that we have employed the {(C$_2$H$_3$O)$_4$}W fragment to investigate the ethylene rearrangements. Calculated geometrical and thermodynamical data obtained for ethylene rearrangements agree with the experimental X-ray data and the observed reaction trend.

1 Introduction

It has been recently reported that an olefin bound to a calix-[4]arene tungsten fragment undergoes a series of rearrangements through deprotonation–protonation reactions which is similar to that shown when coordinated to a metal oxide surface.[1,2] The olefin complex first undergoes a deprotonation leading to anionic metallacyclopropene which then rearranges to an alkylidyne complex, characterised by a triple W–C bond, [{*p*-Bu^t-calix[4](O)$_4$}W≡CMe]$^-$, and may be finally protonated to give the corresponding alkylidene complex, [{*p*-Bu^t-calix-[4](O)$_4$}W=CHCH$_2$R] (see Scheme 1, R = H).

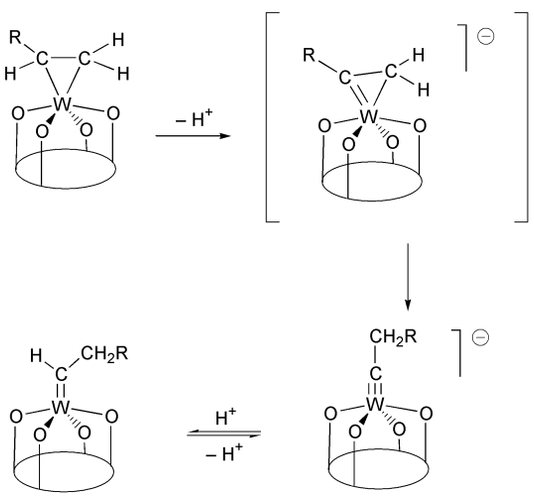

Scheme 1

Some of these systems have been investigated previously at the extended Hückel level with emphasis on a qualitative study of the bonding in the isolated complexes,[1,2] while no previous accurate studies have appeared on this subject. In this paper we carry out a DFT investigation of this olefin rearrangement on the tungsten calix[4]arene fragment. In order to reduce the computational effort, a simplified model of tungsten calix[4]arene is considered, constituted by four vinylate units simulating the phenolate groups of calix[4]arenes. A series of preliminary calculations have shown that such a tetra-vinylate complex allows an accurate description of the calix[4]arene ancillary ligand,[3] taking into account the main geometrical and electronic properties.

We consider the whole pathway leading from the ethylene to the alkylidene complex, characterising the energetics and electronic properties of the reagents, products, and of the possible intermediates of each step. Moreover, we consider in detail the electrophilic attack on alkylidyne, discussing site preference for the attack and characterising the eventual products in accordance with this reactivity.

2 Computational details

The calculations reported in this paper are based on the ADF (Amsterdam Density Functional) program package.[4–6] Its main characteristics are the use of a density fitting procedure to obtain accurate Coulomb and exchange potentials in each SCF cycle, the accurate and efficient numerical integration of the effective one-electron Hamiltonian matrix elements and the possibility to freeze core orbitals. The frozen cores have been 1s–4f for W and 1s for C and O. The molecular orbitals were expanded in an uncontracted double-ζ STO basis set for all atoms with the exception of the transition metal orbitals for which we used a triple-ζ STO basis set for 5d and 6s. As polarisation functions, we used one 3d STO for O and C, a 2p for H, and a 6p for W. Non-local (NL) exchange correlation potentials and energies were used. Becke's non-local correction[7] for the local exchange expression and Perdew's non-local correction[8] for the local expression of correlation energy have been included together with Vosko–Wilk–Nusair parameterisation[9] for homogeneous electron gas correlation. Since the relativistic effects play an important role in describing the electronic structure and relative energetics of the species containing heavy metal, such as tungsten, they were taken into account by the Pauli formalism, the Pauli Hamiltonian

 DOI: 10.1039/b008863n

Table 1 Main computed geometrical parameters of [(calix[4]O_4)W(η^2-C_2H_4)], **1**, compared with data observed for the experimentally obtained compound, and with parameters optimized for the reduced model [{$(C_2H_3O)_4$}W(η^2-C_2H_4)], **1*** (bond lengths in Å and angles in degrees)

	R_{WC}	R_{CC}	R_{WO_1}	R_{WO_2}	$R_{O_1C_1}$	$R_{O_2C_2}$	$\angle O_1WO_3$	$\angle O_2WO_4$	$\angle CWC$
1	2.126	1.452	2.032	1.880	1.369	1.358	164.5	151.2	39.9
1*	2.122	1.450	2.045	1.871	1.345	1.358	165.9	145.9	40.1
Exp.[2]	2.145	1.401	2.030	1.870	1.356	1.373	168.1	152.1	38.1

including first order scalar relativistic corrections (Darwin and mass-velocity) while neglecting spin–orbit corrections.[6,10] Molecular structures of all investigated complexes were optimised at this non-local level including relativistic corrections within symmetry constraints. In order to analyse the [M]–X interaction energies of the investigated complexes, we used an extension[11] of the well known decomposition scheme of Morokuma.[12] The interaction energy ($E_{[M-X]}$) is decomposed into three terms:

$$E_{[M-X]} = -[E^{prep} + E^{ster} + E^{orb}] \quad (1)$$

E^{prep} is the *preparation energy*, the energy necessary to bring the fragments from their ground state equilibrium geometry to the valence state geometry they have in the complex, E^{ster} is the *steric repulsion*, consisting of two components. The first is due to the electrostatic interaction of the nuclear charges and unmodified electronic charge density of one fragment with those of the other fragment, both fragments being at their final positions. The second component is the so-called Pauli repulsion originating from the repulsive interaction between occupied orbitals which is essentially due to the antisymmetry requirement on the total wave function. E^{orb} is the *orbital interaction energy* and can be decomposed, according to the Ziegler scheme,[13] into the energy contributions associated with orbital interactions within the various irreducible representations Γ of the overall symmetry group of the system.

3 Results and discussion

3.1 η^2-C_2H_4 tungsten complex

[{calix[4]$(O)_4$}(η^2-C_2H_4)], **1**, plays a central role in tungsten calix[4]arene reactivity, being the starting reactant in ethylene rearrangements, and has therefore been carefully investigated. The bonding in transition metal complexes of ethylene is usually described by the Dewar–Chatt–Duncanson (DCD) model[14] which has been widely employed to interpret the results of semi-empirical and *ab initio* calculations.[15–17] This model is adequate for donor–acceptor complexes especially with low valence metals, and describes the bond between ethylene and metal moieties as the sum of two independent components: the first is the σ donation from a ligand filled orbital to an empty metal d orbital and the second is the π back-donation from an occupied metal d orbital to the empty ethylene π* orbital. However, the DCD model is an incomplete description of the interaction and does not allow the distinction between pure donor–acceptor interactions and covalent metal–carbon bonds leading to metallacyclopropane species. The d^2 tungsten(IV) {*p*-Bu^t-calix[4]$(O)_4$}W metal fragment is well suited to bind an olefin, as experimentally and theoretically demonstrated.[2] In particular, a previous theoretical investigation on the W(IV) ethylene complex $WCl_4C_2H_4$ has been interpreted in terms of a metallacyclopropane structure rather than a donor–acceptor interaction.[18]

[{calix[4]$(O)_4$}W(η^2-C_2H_4)] has been optimised under the C_{2v} symmetry constraints, and the computed structure is shown in Fig. 1 with the ethylene C–C bond oriented in the *yz* plane. Optimised geometrical parameters and X-ray data have been reported in Table 1: the computed geometry is in good agreement with the experimental structure. The computed structure shows C–C and W–C bond lengths of 1.452 and 2.126 Å, respectively, and a C–W–C angle of 39.9°. The computed C–C distance is much longer than in isolated ethylene (1.332 Å), and approaches the typical values for a C–C single bond (1.54 Å),[19] suggesting a metallacyclopropane description. This is confirmed by the short W–C distance and by the value of the *α* angle (the angle which the C–H bond forms with the plane containing the double C–C bond has been calculated as 10.8°).

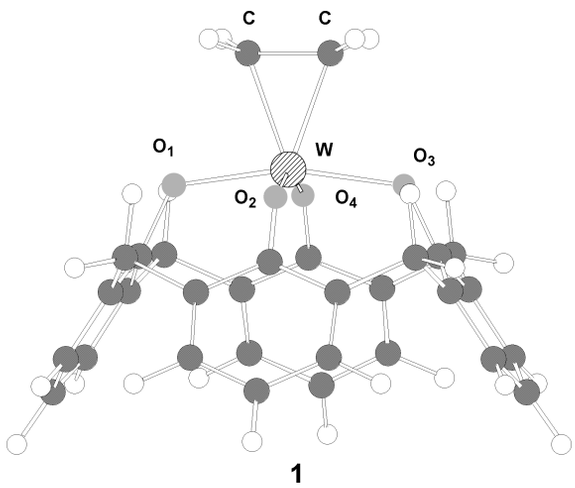

1

Fig. 1 Optimised structure of [{calix[4]$(O)_4$}W(η^2-C_2H_4)], **1**.

The nature of the metal–ligand bonding in **1**, has been analysed in terms of the interaction mode between the ethylene and the metal calixarene fragment in the triplet ground state. Fig. 2 illustrates the orbital interaction diagram of these two fragments in **1**. The ethylene frontier orbitals are shown on the right side, the LUMO is a π_u ($2b_2$) orbital, the anti-bonding combination of carbon p_z orbitals), while the HOMO is a π_g ($3a_1$) orbital (the bonding combination of the same carbon orbitals). Tungsten calix[4]arene frontier orbitals (on the left of Fig. 2) can be described as four low energy localised metal orbitals: $29a_1$ (d_{z^2}), $24b_2$ (d_{yz}) (0.62 eV higher in energy than $29a_1$), $24b_1$ (d_{xz}) and $18a_2$ (d_{xy}) (1.50 eV and 1.57 eV respectively higher in energy than $29a_1$). The empty π_u orbital of ethylene mixes with the $24b_2$ (d_{yz}) metal orbital, giving the $25b_2$ HOMO orbital of the complex, while the filled π_g mixes with the metal $29a_1$ (d_{z^2}) to give a low lying MO. The strong interaction between the two fragments can be ascribed to the good overlap of the π_u orbitals of ethylene and the d_{yz} orbital of tungsten. At the same time the W–O distances in the *yz* plane lengthen due to the decrease in π donation from oxygen atoms to the tungsten d_{yz} orbital.

To evaluate the strength of this interaction we have calculated the bonding energy of **1** according to the bond energy decomposition scheme described above using for the metal fragment the excited singlet state $(29a_1)^2(24b_2)^0$. The results of the energy decomposition, reported in Table 2, shows a peculiar result with a high steric repulsion, 899 kJ mol^{-1}, due essentially to the Pauli contribution (2180 kJ mol^{-1}), which is counterbalanced by an unusually high orbital interaction arising mainly from the B_2 symmetry. This is a physically absurd result and suggests that the electronic structure of this complex cannot be considered as a donor–acceptor interaction but rather as a covalent bond between open shell fragments. The metal fragment has a triplet ground state while ethylene has a singlet ground state and a high excitation energy is lost to reach

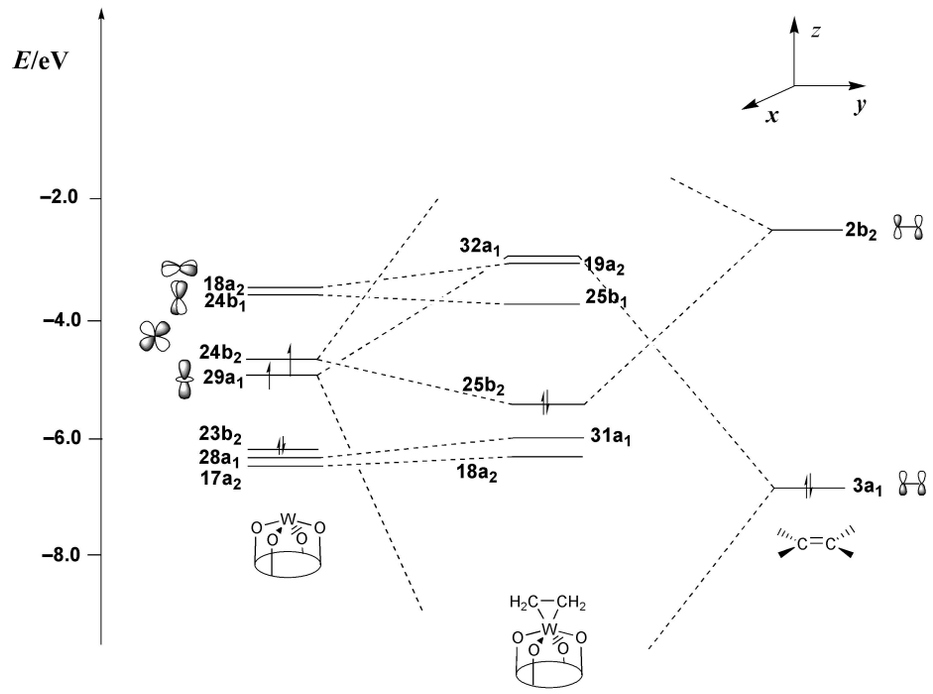

Fig. 2 Orbital interaction diagram for [{calix[4](O)$_4$}W(η^2-C$_2$H$_4$)].

Table 2 Comparison of bonding energy decomposition contributions for **1** and **1*** (kJ mol^{-1})

	E^{ster}	E^{orb}	E^{A_1}	E^{A_2}	E^{B_1}	E^{B_2}	$E^{R}_{C_2H_4}$	$E^{R}_{W(OCH_3H_3)_4}$	$E_{W-C_2H_4}$
1	899	−1149	160	−9	−30	−1271	64	49	137
1*	890	−1165	180	−10	−30	−1306	64	89	113

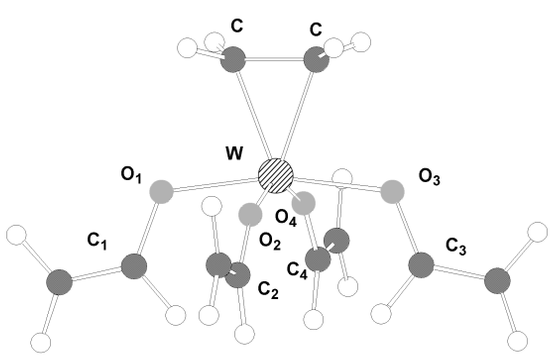

1*

Fig. 3 Optimised structure of [{(C$_2$H$_3$O)$_4$}W(η^2-C$_2$H$_4$)], **1***.

the valence open shell state. This confirms that the bonding between the two fragments is mainly described in terms of a metallacyclopropane description. The calculated overall bonding energy, 137 kJ mol^{-1}, is higher than the typical values for common ethylene metal complexes of group d^{10}, M(PH$_3$)$_2$ (M = Ni, Pd, Pt).[20,21]

3.2 Modeling of the *p*-Bu^t-calix[4]arene ligand

Preliminary calculations were carried out in order to define a simplified model of calix[4]arene which still maintains its main electronic properties. We have considered a few systems of growing complexity (tetra-hydroxides, tetra-ethynylate and tetra-vinylates) finding that four vinylate groups, C$_2$H$_3$O$^-$ arranged as in Fig. 3 reproduce adequately the electronic and structural properties of the whole calix[4]arene ligand.[3] The optimised geometry for [{(C$_2$H$_3$O)$_4$}W(η^2-C$_2$H$_4$)], **1***, is compared in Table 1 with that for the whole complex **1** and shows an excellent agreement. The comparison between the atomic

Table 3 Comparison between Mulliken atomic charges of **1** and **1***

	W	O_1	O_2	C_1	C_2	C_α	H
1	2.670	−0.863	−0.835	0.402	0.378	−0.463	0.081
1*	2.566	−0.869	−0.814	0.350	0.335	−0.471	0.073

Mulliken charges for metal and its first neighbors (Table 3) proves also that the charge distribution is similar in the two complexes, with only minor deviations for the C$_1$ and C$_2$ atoms (bound to oxygen and lying on *xz* and *yz* planes respectively). A comparison between the frontier orbitals of **1** and **1*** also shows similar energies. Moreover, a comparison between the tungsten–ethylene bonding energy and the results of its decomposition for calix[4]arene and tetravinylate, reported in Table 2, also shows very similar results. We can therefore assume that the four vinylate groups adequately reproduce the structural, electronic and energetic properties of the real calix[4]arene ligand and this reduced model is hereafter adopted for investigating the reactive process catalysed by W–calix[4]arene.

3.3 The deprotonation of [{(C$_2$H$_3$O)$_4$}W(η^2-C$_2$H$_4$)] and the formation of alkylidyne

The deprotonation of tungsten–ethylene with LiBu is the main step in the olefin rearrangements assisted by tungsten calixarene.[1] The hydrogen abstraction is favoured by the electron deficient nature of the calixarene supported tungsten(IV) centre which stabilises the resulting carbanions. The alkylidyne is the product of the reaction only if the reactant is a terminal olefin (see Scheme 1). A more detailed experimental study, using the non-terminal olefin stilbene, has shown that deprotonation of [{*p*-Bu^t-calix[4](O)$_4$}W(η^2-CHPhCHPh)] leads to a [{*p*-Bu^t-calix[4](O)$_4$}W(η^2-CHPhCPh)]$^-$ anionic vinyl complex.[1] This result has suggested that an η^2-vinyl species could be a reactive intermediate in the deprotonation of terminal olefins which

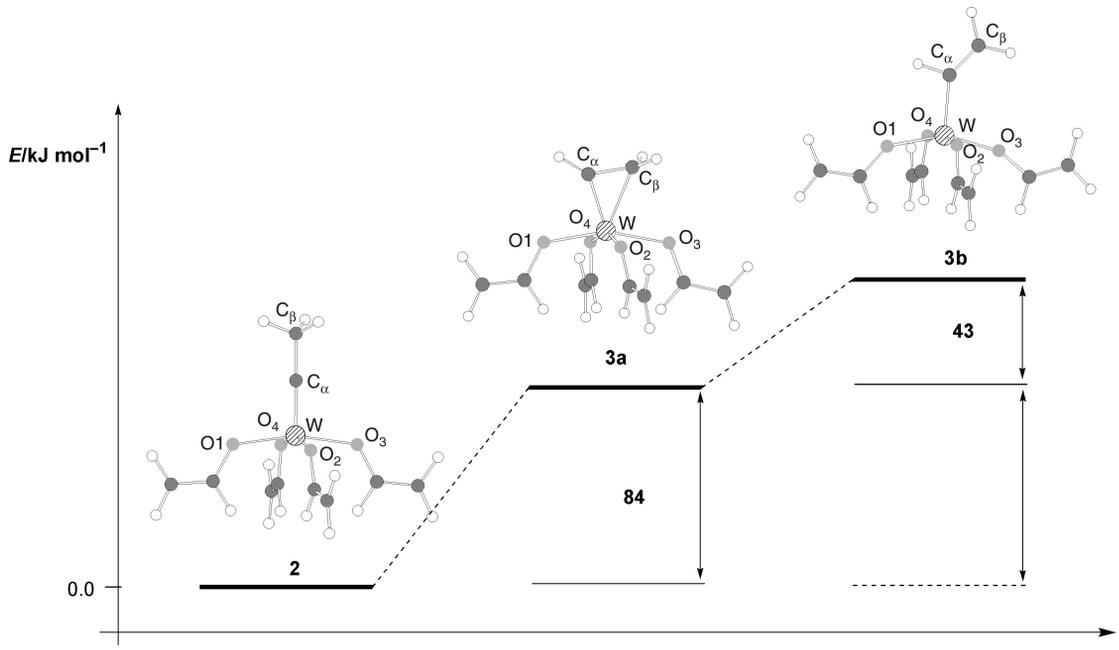

Fig. 4 Optimised structures and relative energies for the three different isomers of $[(OC_2H_3)_4W(C_2H_3)]^-$: **2**, **3a** and **3b**.

Table 4 Main computed geometrical parameters of **2**, **3a**, **4** and **5** and of the corresponding experimental alkylidyne and alkylidene complexes (bond lengths in Å and angles in degrees)

	R_{WC_α}	$R_{C_\alpha C_\beta}$	R_{WC_β}	R_{WO_1}	R_{WO_2}	E_{WO_3}	$\angle O_1WO_3$	$\angle O_2WO_4$	$\angle WC_\alpha C_\beta$
2	1.742	1.467	—	2.032	2.029	2.030	164.2	158.8	179.6
Exp.[1]	1.728	1.445	—	2.000	1.995	1.959	161.7	160.0	173.8
3a	1.886	1.435	2.171	2.047	2.030	2.006	164.2	158.8	40.6
4	1.881	1.497	—	1.891	2.001	1.891	151.9	163.5	131.1
Exp.[1]	1.913	1.437	—	1.853	1.992	1.835	149.3	164.7	135.2
5	1.742	1.463	—	1.945	1.974	2.372	170.3	153.4	172.2

then undergo an irreversible 1,2-proton shift to the corresponding alkylidyne. Transition metal vinyl complexes are usually η^1 coordinated[22,23] and an η^2 coordination has been observed only for coordinatively unsaturated early transition metals.[24] In particular the η^2 coordination in $[\{p\text{-Bu}^t\text{-calix[4](O)}_4\}W\{\eta^2\text{-(CHPhCHPh)}\}]^-$ is probably stabilised because it allows the metal to take four electrons to reach a stable 18 electron configuration.

In order to show that the η^2-vinyl species is a viable intermediate in the deprotonation of the ethylene complex to the corresponding alkylidyne complex, we have optimised (within C_s symmetry) the three complexes: $[\{(OC_2H_3)_4\}W{\equiv}CMe]^-$, **2**, $[\{(C_2H_3O)_4\}W(\eta^2\text{-}C_2H_3)]^-$, **3a**, and $[\{(C_2H_3O)_4\}W(\eta^1\text{-}C_2H_3)]^-$, **3b**. They represent the three different isomers of the same $[\{(OC_2H_3)_4\}W(C_2H_3)]^-$ complex, and their optimised structures and relative stabilities are reported in Fig. 4. The alkylidyne complex is the most stable in agreement with the experimental evidence that this species is the final product of the deprotonation of ethylene complex **1**. Moreover, we see that the η^2-vinyl complex, **3a**, is 43 kJ mol^{-1} more stable than the η^1-vinyl complex, **3b**, confirming the experimental attribution of η^2 coordination to the vinyl complex, based on ^{13}C NMR data. The main geometrical parameters calculated for **2** and **3a** are collected in Table 4 together with the X-ray data for $[\{p\text{-Bu}^t\text{-calix-[4](O)}_4\}W{\equiv}CPh]^-$.[1] The optimised parameters of **2** agree quite well with the experimental data, confirming once again that the model used represents a good approximation. The W–C_α bond distance of **2** is particularly short, 1.742 Å, and falls in the characteristic range for M–C triple bond distances.[25] The tungsten centre shows a square pyramidal coordination, with the four oxygen atoms representing the vertices of the squared basis and the tungsten atom is quasi-coplanar to the oxygens. The complex shows a quasi C_{4v} symmetry, as has been observed for penta-coordinated metals showing a square pyramidal coordination.

Complex **3a** can be described as a tungstenacyclopropene characterised by two asymmetric W–C_α and W–C_β bonds, 1.886 and 2.171 Å, corresponding to a double and a single tungsten–carbon bond respectively; the C_α–C_β distance, 1.435 Å, is close to the value of single C–C bonds. Both metal–carbon and carbon–carbon distances are close to those observed in similar metallacyclopropene complexes of tungsten and molybdenum.[26]

In order to adequately explain the nature of the W–C interaction in the investigated complexes, we have analysed the electronic structures of **2** and **3a** in terms of the $\{(C_2H_3O)_4\}W^-$ and C_2H_3 fragments in their lowest electronic states. The diagrams of molecular orbital interactions for **2** and **3a** are shown respectively in Figs. 5 and 6 where we draw the metal fragment orbitals on the left and those of the organic fragments on the right. In both cases the metal fragment has a quartet ground state with the 31a′, 18a″ and 32a′ singly occupied. In the alkylidyne, see Fig. 5, the C_2H_3 fragment has a doublet ground state with the 2a″ orbital singly occupied. The 2a″ and 5a′ orbitals (essentially the p_x and the p_y of C_α) mix with the two highest singly occupied orbitals of the metal fragment, 18a″ (d_{xz}) and 32a′ (d_{yz}), giving the two highest occupied MOs of alkylidyne, 19a″ and 35a′. These two MOs are near degenerate and describe the W–C π bonds in the perpendicular *yz* and *xz* planes confirming the triple bond nature of W–C. The σ interaction is very low in energy and derives from the interaction between the 31a′ orbital of the metal fragment (30% s + 68% d_{z^2} of W) and the 4a′ orbital of the organic moiety (33% 2s + 48% $2p_z$ of C_α). This picture is in agreement with the current description of bonding in Schrock alkylidynes as covalent bonds between open shell fragments; the metal

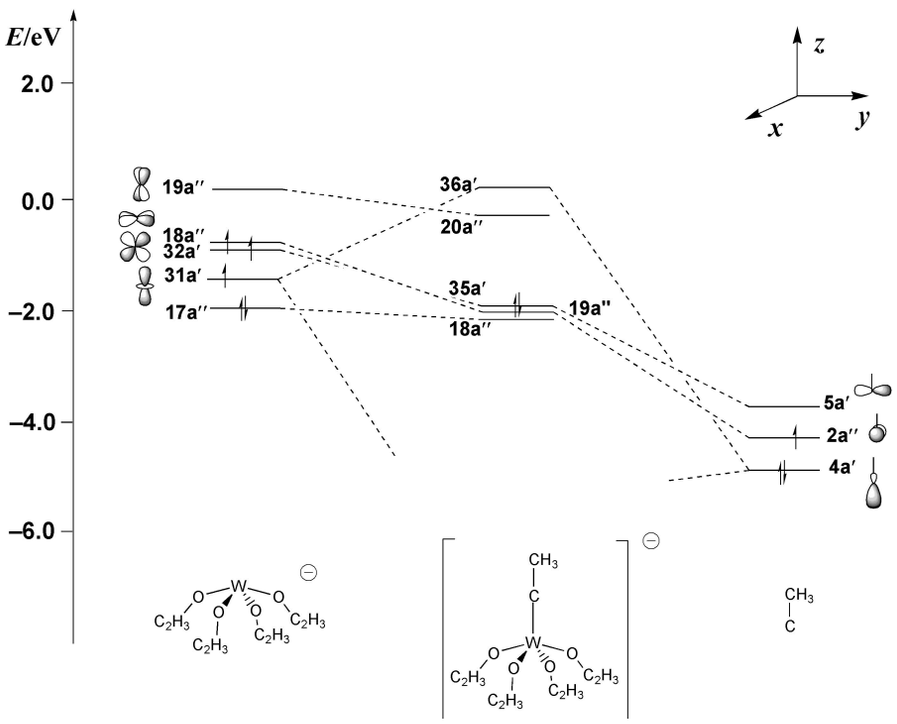

Fig. 5 Orbital interaction diagram for $[\{(OC_2H_3)_4\}W{\equiv}CMe]^-$.

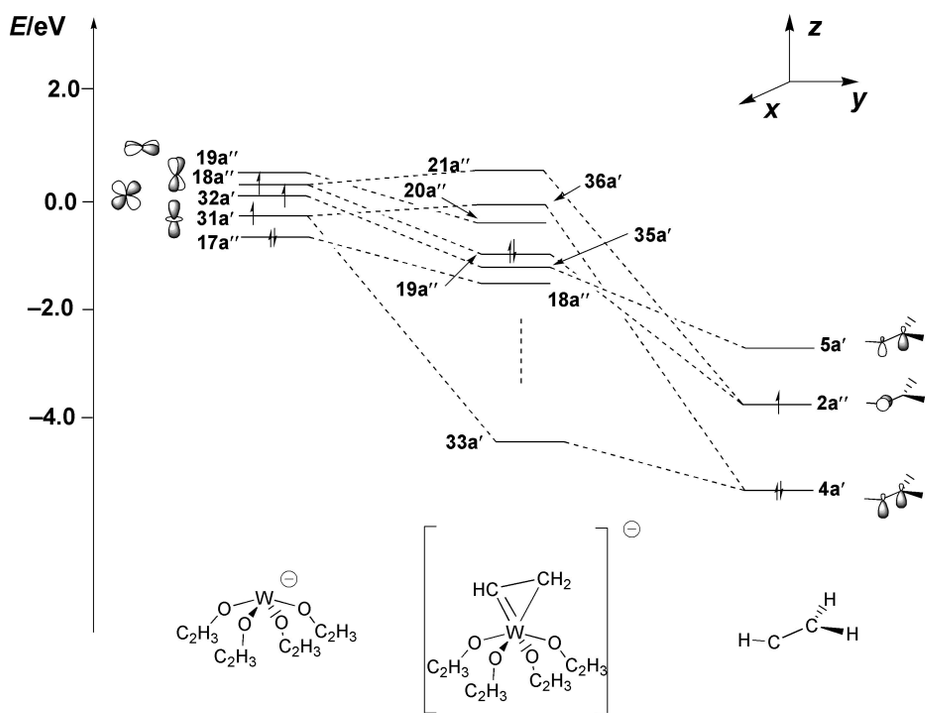

Fig. 6 Orbital interaction diagram for $[\{(C_2H_3O)_4\}W(\eta^2\text{-}C_2H_3)]^-$.

fragment is already in the quartet valence state while the organic fragment requires a relatively small excitation energy to reach its valence quartet state. The computed dissociation energy is quite large, 613 kJ mol^{-1}, as expected for a triple metal carbon bond.

Fig. 6 illustrates the orbital interaction diagram for **3a**. The main frontier orbitals of the $CHCH_2$ moiety in its lowest doublet state are the doubly occupied 4a′ (a bonding combination of C_α and C_β p_z orbitals, rehybridised to point towards the metal), the singly occupied 2a′′ (essentially the C_α p_x orbital of $\pi_\perp$ character) and the empty 5a′ (the corresponding antibonding combination of C_α and C_β p_z orbitals). The molecular orbitals describing the fragments interactions are: 33a′ which is the bonding combination of the 31a′ (d_{z^2}) orbital of the metal moiety and the 4a′ orbital of the vinyl moiety; 35a′ which is the bonding combination of 32a′ (d_{yz}) with 5a′; 19a′′ which is the bonding combination of 18a′′ (d_{xz}) and 2a′′($\pi_\perp$). The two orbitals of A′ symmetry describe the "in plane" W–C interactions while the 19a′′ orbital describes essentially a π interaction between W and C_α, as expected for a metallacyclopropene structure. As in **2** the electronic structure of **3a** can be described in terms of covalent bonds between open shell (quartet and doublet) fragments. In **3a** the W–O bonds in the *yz* plane (containing the vinyl unit) are longer than those in the orthogonal *xz* plane because the d_{yz} orbital is engaged in π interactions with the vinyl unit and are less available to the π donation from the calixarene oxygens. The final bonding energy is 321 kJ mol^{-1}.

3.4 The protonation of $[\{(OC_2H_3)_4\}W{\equiv}CMe]^-$ and the formation of alkylidene

The reversible protonation of the alkylidyne leads to the corresponding alkylidene (see Scheme 1), which can therefore be considered as the final product of the ethylene rearrangement assisted by tungsten calix[4]arene. The optimised structure of $[\{(OC_2H_3)_4\}WC(H)Me]$, **4** is shown in Fig. 7 and the main bond lengths and angles are compared with the X-ray data for $[\{p\text{-Bu}^t\text{-calix[4](O)}_4\}W{=}C(H)Ph]$[1] in Table 4. The computed geometrical parameters match quite well with the experimental data, taking into account that we refer to an alkylidene with a methyl group instead of a phenyl group as in the experimental compound. It is to be noted that the calculated W–C_α distance, 1.881 Å, is quite close to the experimental value of 1.913 Å and falls in the range for W–C double bond distances. At the same time our calculations reproduce alternations in W–O bond length, with the mean value of the W–O_1 and W–O_3 distances, in the alkylidene plane, shorter than the values of the W–O_2 distances. The electronic structure of $[\{(OC_2H_3)_4\}WC(H)Me]$ has been analysed in terms of the interaction between the $\{(C_2H_3O)_4\}W$ and $C(H)CH_3$ fragments in their lowest triplet states. On the left of Fig. 8 are reported tungsten fragment orbitals, while on the right are the frontier orbitals of the alkylidene unit. These are the singly occupied 5a′, a C_α hybrid (s + p_z) pointing towards the metal, and 2a″, a C_α p_x orbital of $\pi_\perp$ character. The main bonding interactions are described by 33a′ and 19a″, the HOMO. The former is very low in energy and is the σ bonding combination of 31a′ and 5a′; the latter is the bonding combination of 18a″ and 2a″ and has a relevant π character in the *xz* plane. This bonding π interaction engages the d_{xz} orbital which is no longer available for π donation from the calixarene oxygen thus leading to a lengthening of the W–O_2 bond lengths in the *xz* plane perpendicular to the alkylidene unit. Here again the electronic structure of **4** can be described in terms of covalent bonds between open shell (triplet) fragments. The calculated bonding energy is 464 kJ mol^{-1}.

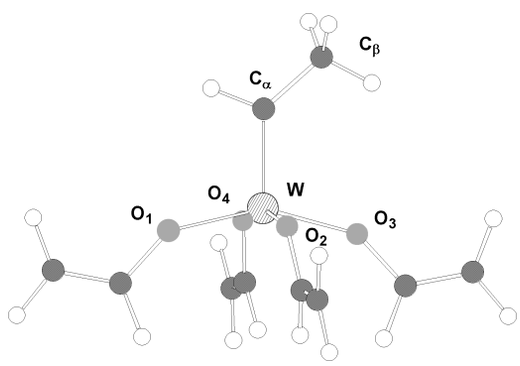

4

Fig. 7 Optimised structure of $[\{(OC_2H_3)_4\}WC(H)Me]$, **4**.

3.5 Attack of hard electrophiles on the alkylidyne complex

The alkylidyne complex is an electron rich species and easily undergoes an electrophilic attack. The electrophilic attack on $[\{p\text{-Bu}^t\text{-calix[4](O)}_4\}W{\equiv}CR]^-$ (R = Ph, Pr) has been experimentally investigated using different electrophiles like H^+ and Me^+.[1] The reversible protonation of these alkylidyne complexes occurs only at the alkylidyne carbon atoms (C_α) and leads to the corresponding alkylidene species; on the other hand the methylation (by MeOTf) of these alkylidynes may involve either the alkylidynic carbon or the calixarene oxygens thus leading to a mixture of two products, in similar amounts, *i.e.* the corresponding alkylidene and the alkylidyne based on a methylated calixarene fragment. The regiochemistry of the electrophilic attack may be determined by both charge and frontier orbital factors, and charge effects are expected to be important for these anionic alkylidyne species, especially when hard electrophiles such as H^+ and Me^+ are considered.[1] The results of the Mulliken charges analysis on $[\{(OC_2H_3)_4\}W{\equiv}CMe]^-$, see Table 5, show that the oxygen atoms and the alkylidyne carbon have by far the highest negative charges with similar values (−0.84 and −0.74) so that the incoming electrophiles are expected to attack both oxygen and carbon. This hypothesis agrees well with the regiochemistry experimentally observed for Me^+ attack illustrated in Scheme 2.

The protonation of $[\{p\text{-Bu}^t\text{-calix[4](O)}_4\}W{\equiv}CR]^-$ (R = Ph) with py·HCl leads, instead, exclusively to alkylidenes, but this result could be due to the high mobility of the proton which may migrate easily from the oxygen to the carbon atom giving the thermodynamically most stable product.

In order to check this point we have considered also the other possible product of the reaction of the alkylidyne with H^+, the O-protonated alkylidyne, $\{(C_2H_3O)_3(C_2H_3OH)\}WCCH_3$, **5**.

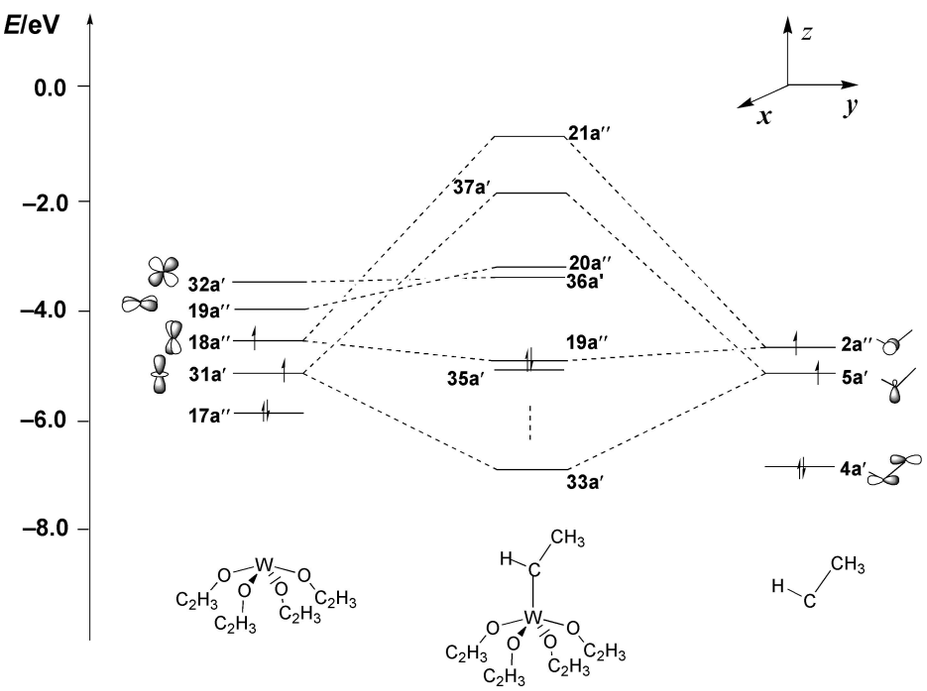

Fig. 8 Orbital interaction diagram for $[\{(OC_2H_3)_4\}WC(H)Me]$.

Table 5 Mulliken atomic charges of $[\{(OC_2H_3)_4\}W{\equiv}CMe]^-$, **2**, $[\{(C_2H_3O)_4\}W(\eta^2\text{-}C_2H_3)]^-$, **3a**, and $[\{(OC_2H_3)_4\}WC(H)Me]$, **4**

	W	O_1	O_2	O_3	C_1	C_2	C_3	C_α	C_β
2	2.18	−0.84	−0.84	−0.84	0.39	0.38	0.39	−0.74	−0.11
3a	2.40	−0.82	−0.84	−0.83	0.37	0.35	0.36	−0.53	−0.44
4	2.50	−0.86	−0.83	−0.86	0.36	0.35	0.34	−0.79	−0.11

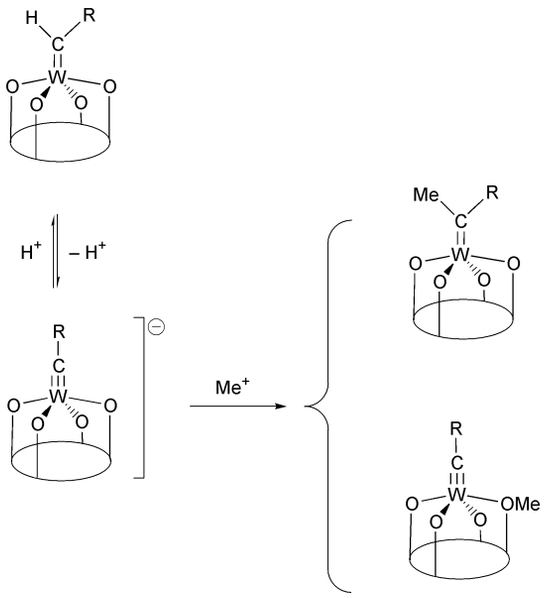

Scheme 2

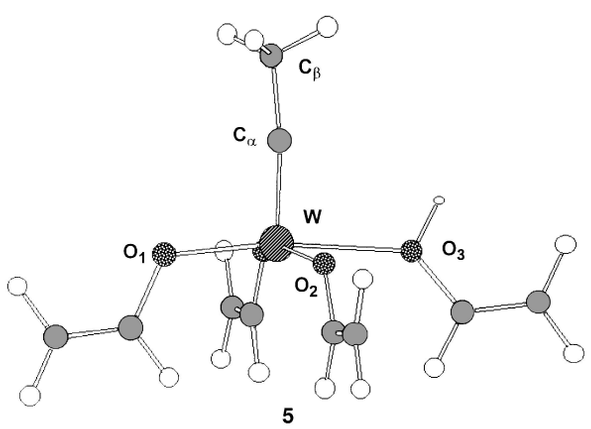

5

Fig. 9 Optimised structure of $\{(C_2H_3O)_3(C_2H_3OH)\}WCCH_3$, **5**.

The optimised structure, constrained to have C_s symmetry, is shown in Fig. 9 and shows a remarkable distortion of the alkylidyne unit with a W–C_α–C_β angle of 172.2°. The W–O_3 distance, with the protonated vinylate ligand, is longer than the corresponding W–O bonds with the other three vinylates, as expected from the different nature of the oxygen atoms. It is worth noting that alkylidene complex **4** is 114 kJ mol^{-1} more stable than the O-protonated alkylidyne complex **5**, and is therefore the thermodynamically most stable product of the protonation of the alkylidyne complex **2**. From the comparison of the starting reactant and the final product energy it emerges that the alkylidene is 9 kJ mol^{-1} more stable than the η^2-C_2H_2 tungsten complex. We can conclude that the thermodynamic product of the ethylene rearrangement on the tungsten fragment, through deprotonation and protonation pathways, is the alkylidene complex.

4 Conclusions

We have investigated by DFT methods the complexes involved in the rearrangements undergone by ethylene bound to a calix[4]arene tungsten fragment. Within this study we have shown the possibility of describing the complex reactivity of the W–calix[4]arene with the $\{(C_2H_3O)_4\}W$ reduced model. Indeed, from the comparison between geometrical, electronic and bonding parameters of $[\{p\text{-Bu}^t\text{-calix[4](O)}_4\}W(\eta^2\text{-}C_2H_4)]$ and $[\{(C_2H_3O)_4\}W(\eta^2\text{-}C_2H_4)]$ we may conclude that four vinylate groups represent a good approximation for the calix[4]arene ligand. We have also investigated the olefin rearrangements occurring on calix[4]arene tungsten using this reduced model. All complexes involved in these reactions have been characterised, and the calculated geometries and thermodynamics agree with the experimental X-ray data and the observed reaction trend. The final methyl alkylidene product is the thermodynamically most stable species and lies 9 kJ mol^{-1} below the starting ethylene tungsten complex. The protonation of the anionic alkylidyne intermediate, directed to the alkylidynic carbon, is found to be driven by thermodynamics and leads to the energetically most stable alkylidene product. Moreover our results confirm that the deprotonation of the metal bound olefin to the alkylidyne complex occur *via* the intermediacy of an η^2-vinyl species which then undergoes a 1,2-proton shift.

Acknowledgements

The present work has been carried out in the context of the COST D9 Action. Thanks are due to the CNR (Progetto Finalizzato "Materiali Speciali per Tecnologie Avanzate II") for financial support.

References

1 L. Giannini, E. Solari, S. Dovesi, C. Floriani, N. Re, A. Chiesi-Villa and C. Rizzoli, *J. Am. Chem. Soc.*, 1999, **121**, 2784.
2 L. Giannini, G. Guillemot, E. Solari, C. Floriani, N. Re, A. Chiesi-Villa and C. Rizzoli, *J. Am. Chem. Soc.*, 1999, **121**, 2797.
3 S. Fantacci, Ph.D. Thesis, University of Perugia, 1998.
4 E. J. Baerends, D. E. Ellis and P. Ros, *Chem. Phys.*, 1973, **2**, 42; E. J. Baerends and P. Ros, *Chem. Phys.*, 1973, **2**, 51; E. J. Baerends and P. Ros, *Chem. Phys.*, 1975, **8**, 41; E. J. Baerends and P. Ros, *Int. J. Quantum Chem.*, 1978, **S12**, 169.
5 P. M. Boerrigter, G. te Velde and E. J. Baerends, *Int. J. Quantum Chem.*, 1988, **33**, 87; G. te Velde and E. J. Baerends, *J. Comput. Phys.*, 1992, **99**, 84.
6 T. Ziegler, V. Tshinke, E. J. Baerends, J. G. Snijders and W. Ravenek, *J. Phys. Chem.*, 1989, **93**, 3050.
7 A. D. Becke, *Phys. Rev. A*, 1988, **38**, 2398.
8 J. P. Perdew, *Phys. Rev.*, 1986, **33**, 8822.
9 S. H. Vosko, L. Wilk and M. Nusair, *Can. J. Phys.*, 1990, **58**, 1220.
10 P. M. Boerrigter, Ph.D. Thesis, Vrije University, 1987; J. Li, G. Schreckenbach and T. Ziegler, *J. Am. Chem. Soc.*, 1995, **117**, 486 and references therein.
11 E. J. Baerends, in *Cluster Models for Surface and Bulk Phenomena*, ed. G. Pacchioni and P. S. Bagus, Plenum Press, New York, 1992, pp. 189–207.
12 K. Morokuma, *J. Chem. Phys.*, 1971, **55**, 1236; K. Kitaura and K. Morokuma, *Int. J. Quantum Chem.*, 1976, **10**, 325.
13 T. Ziegler and A. Rauk, *Theor. Chim. Acta*, 1977, **46**, 1.
14 (*a*) M. J. S. Dewar, *Bull. Soc. Chim. Fr.*, 1951, **18**, C71; (*b*) J. Chatt and L. A. Duncanson, *J. Chem. Soc.*, 1953, 2939.
15 T. A. Albright, R. Hoffmann, J. C. Thibeault and D. L. Thorn, *J. Am. Chem. Soc.*, 1979, **101**, 3801.
16 T. Ziegler and A. Rauk, *Inorg. Chem.*, 1979, **18**, 1558.
17 K. Kitaura, S. Sakaki and K. Morokuma, *Inorg. Chem.*, 1981, **20**, 2292.
18 G. Frenking and U. Pidun, *J. Chem. Soc., Dalton Trans.*, 1997, 1653; G. Frenking and U. Pidun, *Organometallics*, 1995, **14**, 5325.

19 S. W. Benson, in *Thermochemical Kinetics*, Wiley-Interscience, New York, 2nd edn., 1976, p. 60.
20 J. Li, G. Schreckenbach and T. Ziegler, *Inorg. Chem.*, 1995, **34**, 3245.
21 F. Nunzi, A. Sgamellotti, N. Re and C. Floriani, *J. Chem. Soc., Dalton Trans.*, 1999, 3487.
22 P. T. Wolczansky and J. E. Bercaw, *Acc. Chem. Res.*, 1980, **13**, 121.
23 J. M. Manriquez, P. J. Fagan, T. J. Marks, C. S. Day and V. W. Day, *J. Am. Chem. Soc.*, 1987, **100**, 7112.
24 S. R. Allen, R. G. Beevor, M. Green, N. C. Norman, A. G. Orpen and I. D. Williams, *J. Chem. Soc., Dalton Trans.*, 1985, 435.
25 W. E. Buhro and M. H. Chisholm, *Adv. Organomet. Chem.*, 1987, **27**, 311.
26 J. L. Davidson, M. Shivalian, L. M. Muir and K. W. Muir, *J. Chem. Soc., Chem. Commun.*, 1979, 30; J. L. Davidson, I. E. P. Murray, P. N. Preston, M. V. Russo, L. M. Muir and K. W. Muir, *J. Chem. Soc., Chem. Commun.*, 1981, 1059; J. L. Davidson, G. Vasapollo, L. M. Muir and K. W. Muir, *J. Chem. Soc., Chem. Commun.*, 1982, 1025.